Generation of swirl due to symmetry breaking

V. Shtern, M. Goldshtik, and F. Hussain
Department of Mechanical Engineering, University of Houston, Houston, Texas 77204-4792
(Received 7 September 1993)

We study symmetry breaking in a meridional steady motion of viscous incompressible fluids by considering the case of a laminar axisymmetric "vortex dynamo." Using a linear and subsequently a nonlinear analysis we demonstrate the feasibility of a supercritical pitchfork birfurcation from an initially "trivial" nonswirling flow solution to one with a steady (clockwise or counterclockwise) swirling regime as the Reynolds number exceeds a critical value. This agrees with recent experimental results for a flow inside a conical meniscus, as observed in electrosprays.

PACS number(s): 47.15.−x, 47.20.Ky

I. INTRODUCTION

The appearance of swirl in initially nonswirling flows due to some instability is a striking and intriguing case of symmetry breaking. Conservation of angular momentum implies that the generation of swirl is possible only if spatially separated regions of positive and negative angular momenta (with zero total) are formed. When the negative (or positive) angular momentum is either transferred to ambient bodies or diffused to infinity, the positive (or negative) part becomes dominant in the fluid motion. The direction of rotation (clockwise or counterclockwise) is determined purely by the initial disturbances.

Swirl generation as a result of symmetry breaking can take place in the formation of strong atmospheric vortices, flow in a bathtub, whirlpools, and rotational motion of astrophysical objects. It has also been observed in several experiments. Torrance [1] studied thermal convection in a sealed can with a temperature gradient along the sidewall corresponding to stable stratification and a local source of heat at the center of the can bottom. In this case, a pure meridional circulation develops and an ascending jet is formed near the axis. At certain parameter values, the jet undergoes symmetry breaking and begins to rotate. Another example is the flow into a sink located at the center of the bottom surface of a rectangular box [2]. In this case, a swirling motion is observed when the flow rate exceeds a threshold. The motion of surface waves in a glass of water oscillated horizontally along a straight line [3] becomes rotational at certain values of amplitude and frequency of oscillation.

More recently, generation of swirl has been noted in Zeleny-Taylor cones [4]. Zeleny [5] found that the meniscus of a conducting liquid at the exit of a capillary tube becomes conical when the tube is charged to a sufficiently high potential. Taylor [6] explained the conical nature of the meniscus to be due to a balance between electrical pressure and surface tension action when the liquid is at rest. In the vicinity of the cone apex (of a length scale three orders of magnitude lower than the capillary diameter), the liquid surface is disrupted and a thin jet or spray erupts. Experiments [7] have shown that, contrary to earlier conjectures, the flow inside the cone is circulatory and not unidirectional. Finally, Fernandez de la Mora, Feria, and Barrero [4] "have made numerous observations of vigorous swirl inside Taylor cones, for which there appears to be no obvious external forcing."

Theoretical predictions of spontaneous rotation to date have been related to unsteady motions [3,8] or turbulence [9,10]. In this paper, using bifurcation analysis of steady solutions of the Navier-Stokes equations, we demonstrate that swirl can be generated in an axisymmetric laminar flow.

II. PROBLEM FORMULATION

We consider steady flow of a viscous incompressible fluid that possesses a conical similarity and admits the representation:

$$\begin{aligned} v_r &= -\nu\psi'(x)/r \ , \\ v_\theta &= -\nu\psi(x)/(r\sin\theta) \ , \\ v_\phi &= \nu\Gamma(x)/(r\sin\theta) \ , \\ p &= p_\infty + \rho\nu^2 q(x)/r^2 \ , \\ \Psi &= \nu r\psi(x) \ , \\ x &= \cos\theta \ . \end{aligned} \tag{1}$$

Here, (r,θ,ϕ) are spherical coordinates; r is the distance from the origin; θ and ϕ are polar and azimuthal angles (Fig. 1); v_r, v_θ, v_ϕ, p, ρ, and Ψ are the velocity components, pressure, density, and Stokes stream function, respectively; and ψ, Γ, and q are dimensionless stream function, circulation, and pressure (the prime denotes differentiation with respect to x).

The Navier-Stokes equations allow solutions of the form (1) and can be transformed to a system of sixth-order ordinary differential equations (ODE's) given by

$$(1-x^2)^2\psi^{\mathrm{IV}} - 4x(1-x^2)\psi''' = 2\Gamma\Gamma' + \tfrac{1}{2}(1-x^2)(\psi^2)''' \ , \tag{2}$$

and

$$(1-x^2)\Gamma'' = \psi\Gamma' \ . \tag{3}$$

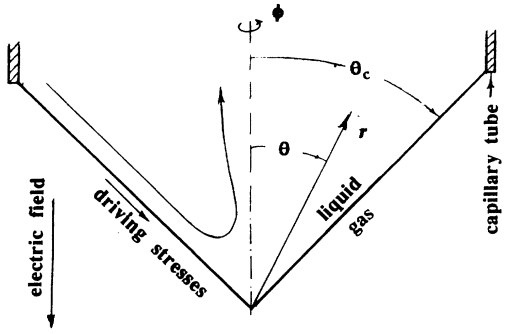

FIG. 1. Schematic of the problem. Coordinates, a typical streamline, and shear stresses are shown.

At the cone surface, i.e., $x=x_c$, the boundary conditions are

$$\psi=0 , \tag{4a}$$

$$\psi'=\mathrm{Re} , \tag{4b}$$

and

$$\Gamma'+2\Gamma x_c/(1-x_c^2)=0 . \tag{4c}$$

At the flow axis, i.e., $x=1$,

$$\psi=0 , \tag{5a}$$

$$\psi' \text{ is bounded} , \tag{5b}$$

and

$$\Gamma=0 . \tag{5c}$$

Equation (4a) represents the impermeability of the cone boundary, and (4b) introduces the Reynolds number $\mathrm{Re}=-rv_{rc}/\nu$; v_{rc} is the radial velocity at the cone surface and the negative sign is chosen to ensure that Re is positive for a flow converging to the apex along the surface. Re characterizes the intensity of the meridional motion which is driven by the radial shear stress

$$\tau_{\theta r}=2\,\mathrm{Re}(1+x_c)\rho\nu^2(r^2\sin\theta)^{-1} .$$

Condition (4c) implies the absence of the azimuthal shear stress

$$\tau_{\theta\phi}=[\Gamma'+2\Gamma x_c/(1-x_c^2)]\rho\nu^2/r^2 .$$

Figure 1 also shows a schematic of the basic meridional flow. It is convenient to introduce an auxiliary function F satisfying

$$(1-x^2)F'''=2\Gamma\Gamma' . \tag{6}$$

After division by $(1-x^2)$, Eq. (2) may be integrated three times to obtain

$$(1-x^2)\psi'+2x\psi-\tfrac{1}{2}\psi^2=F . \tag{7}$$

Using the conditions from (5) in the above equation, we find

$$F(1)=F'(1)=0 . \tag{8}$$

Equation (3) with conditions (4) and (5) has the trivial solution $\Gamma\equiv0$. Our goal is to find a nontrivial solution.

III. SOLUTION OF THE LINEAR PROBLEM

The necessary condition for a bifurcation with swirl to occur is for the problem [(3), (4c), and (5c)] to have a nonzero solution at a given ψ when the influence of Γ (a measure of swirl) on ψ is neglected. As the value of ψ has to be prescribed, its nature itself needs to be analyzed first. To simplify Eq. (7), we introduce a new variable T, such that

$$\psi=-2(1-x^2)T'/T . \tag{9}$$

For $\Gamma\equiv0$, from (4b), (6), (7), and (8), $F=\mathrm{Re}_c(1-x)^2$, where

$$\mathrm{Re}_c=\mathrm{Re}(1+x_c)/(1-x_c) .$$

Therefore, (7) reduces to

$$T''+\tfrac{1}{2}F(1-x^2)^{-2}T=0 , \tag{10a}$$

with the conditions

$$T(x_c)=1, \quad T'(x_c)=0 . \tag{10b}$$

The first condition in (10b) allows T to be normalized to unity, while the second follows from (4a) and (9). Substituting (9) in (3) and integrating once, we get $\Gamma'=\Gamma'(x_c)T^{-2}$. For the linear problem, the normalization $\Gamma(x_c)=1$, together with (4c), yields

$$S(\mathrm{Re})\equiv\Gamma(1)=1-2x_c(1-x_c^2)^{-1}\int_{x_c}^{1}T^{-2}dx . \tag{11}$$

Thus, (5c) gives the condition for swirl generation: $S(\mathrm{Re})=0$. Since at $\mathrm{Re}=0$, $F\equiv0$ and $T\equiv1$, it follows from (11) that

$$S(0)=(1-x_c)/(1+x_c)>0$$

because $|x_c|<1$. Thus, Re_* is the value of Re for which $S(\mathrm{Re})$ changes sign. It is evident from (11) that this does not occur when $x_c\le0$. Now we show that S changes sign for some $x_c\ge0$.

To achieve this, we introduce $F_1=(1+x)^2F/4$ and note that $F_1<F$ because $x<1$. Then, replacing F by F_1 in (10) yields

$$T_1''+(\mathrm{Re}_c/8)T_1=0 , \quad T_1(x_c)=1 , \quad \text{and} \quad T_1'(x_c)=0 , \tag{12}$$

which has the solution

$$T_1(x)=\cos[(\mathrm{Re}_c/8)^{1/2}(x-x_c)] .$$

$T_1(x)$ has a zero inside the interval $(x_c,1)$ when

$$\mathrm{Re}>\mathrm{Re}_1^*=2\pi^2/(1-x_c^2) .$$

Let us define $\psi_1(x)$ to be the solution of (2) with F replaced by F_1 and the same initial condition, $\psi_1(x_c)=0$. From the theorem on differential inequalities, $\psi_1(x)\ge\psi(x)$. The integral form of (9) gives

$$T(x)=\exp\left[-\int_{x_c}^{x}\psi(x)(1-x^2)^{-1}dx\right] .$$

For $T(x) \leq T_1(x)$, there exists a $\mathrm{Re}^* \leq \mathrm{Re}_1^*$; hence, $T(x)$ has a zero inside the interval $(x_c, 1)$, when $\mathrm{Re} > \mathrm{Re}^*$. It is clear from (11) that as $\mathrm{Re} \to \mathrm{Re}^*$, $S(\mathrm{Re}) \to -\infty$. Since $S(\mathrm{Re})$ is a continuous function of Re for $\mathrm{Re} < \mathrm{Re}^*$, there exists an $\mathrm{Re}_* < \mathrm{Re}^*$ for which $S=0$. This completes the proof.

Numerically, the linear problem is solved by integrating (3) and (7) for a given $F = \mathrm{Re}_c(1-x)^2$ from $x=x_c$ to $x=1$ as an initial-value problem with the initial conditions: $\psi(x_c)=0$, $\Gamma(x_c)=1$, and

$$\Gamma'(x_c) = -2x_c/(1-x_c^2) .$$

At $x=1$, conditions (5a) and (5b) are automatically satisfied, and we look for a $\mathrm{Re}=\mathrm{Re}_*$ at a fixed x_c when $\Gamma(1)$ becomes zero. Also, we integrate (10) up to the first zero x_1 of $T(x)$. For small Re, $x_1 > 1$; x_1 decreases as Re increases, and we look for $\mathrm{Re}=\mathrm{Re}^*$ when $x_1 = 1$.

Figure 2 shows the results of numerical calculations of Re_* and Re^* as functions of x_c. As Re approaches Re^*, the so-called "collapse" of meridional flow occurs [10] when the axial velocity becomes infinite as convergent convective transport of axial momentum dominates over viscous diffusion. Thus, the curve $\mathrm{Re}^*(x_c)$ is the boundary of existence of regular nonswirling solutions; for $\mathrm{Re} \geq \mathrm{Re}^*$, there is the sink-type singularity on the axis [10]. However, at a smaller value of Re, i.e., $\mathrm{Re}=\mathrm{Re}_*$, the swirling regime bifurcates and the flow avoids the collapse (shown in Fig. 5). The $\mathrm{Re}_*(x_c)$ curve is terminated where it meets the curve $\mathrm{Re}^*(x_c)$ at $x_c=0$; this agrees with the above result that self-rotation is impossible for $x_c \leq 0$.

The following numerical calculations are made for a cone angle $\theta_c = 45°$ (i.e., $x_c = 0.707$). This angle is chosen not only because it is the mean of the limiting cases (0° and 90°), but also because it is within the range of most experiments of liquid menisci in electrosprays. Although

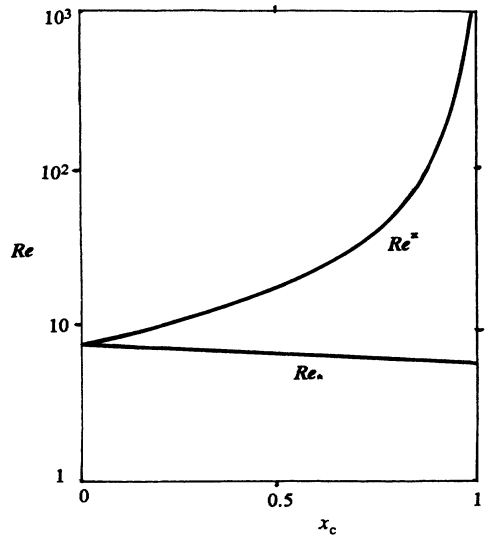

FIG. 2. The critical Reynolds numbers for the self-rotation (Re_*) and collapse (Re^*) versus x_c, where $x_c = \cos^{-1}(\theta_c)$. θ_c is the cone angle.

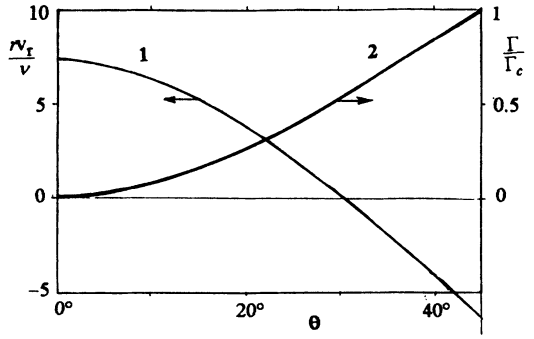

FIG. 3. Angular distributions of the radial velocity of the primary flow (1) and the neutral disturbances of circulation (2) at $\mathrm{Re}=\mathrm{Re}_*$. $\theta_c = 45°$.

Taylor predicted $\theta_c = 49.3°$ for the equipotential surface of highly conducting liquids (at rest), the experimentally observed range is $32° < \theta_c < 46°$; the variation is due to the influence of charged droplets [11].

Figure 3 shows the dependence of the dimensionless radial velocity rv_r/ν (curve 1) and circulation for a perturbed neutral state (curve 2) on the polar angle θ for a primary nonswirling flow at $\mathrm{Re}=\mathrm{Re}_*=6.3$. Both functions are smooth and monotonic with moderate derivatives, thus showing that the case is far from being singular (for example, at $x_c = 0.707$ in Fig. 2).

IV. SOLUTION OF THE NONLINEAR PROBLEM

To solve the nonlinear problem, we integrate the system (3), (6), and (7) as an initial-value problem from $x=1$ to $x=x_c$ by adding the the condition (5) and starting with tentative values of $\psi'(1)$, $\Gamma'(1)$, and $F''(1)$. Note that, due to singularity, $\psi'(1)$ cannot be found from (7) and has to be prescribed (for details, see [10] where system (3), (6), and (7) and its solutions were studied in another context). Then, using the shooting method, we choose $\psi'(1)$ and $F''(1)$ to satisfy $\psi=0$ and (4c) at $x=x_c$. The value of $\Gamma'(1)$ remains a free parameter which implicitly defines Re. For $\Gamma'(1) \ll 1$, the solution of the nonlinear problem is almost the same as the linear one. Therefore, we use the results of the linear problem to start the shooting procedure and iterate till convergence is achieved.

Figure 4 shows the dependence of $\Gamma_c = \Gamma(x_c)$ on Re (curve 2). Line 1 corresponding to the primary solution is shown by a dashed line for $\mathrm{Re} > \mathrm{Re}_*$ because we expect it to become unstable after bifurcation. As the abscissa in Fig. 4 is the line of symmetry, we have supercritical pitchfork bifurcation of the secondary regime. The other two curves in Fig. 4 relate to the problem when both Γ_c and Re are given but condition (4c) is omitted. Curve 4 indicates the collapse boundary, to the right of which the solution is singular. Curve 3 is the boundary between one- and two-cell regimes; the sketches below and above the curve illustrate the meridional flow. The swirling regime remains unicellular near the bifurcation point as long as curve 2 is below curve 3. At the point of intersection of the two curves, an internal flow separation occurs at the cone axis. As Re is increased further, an additional

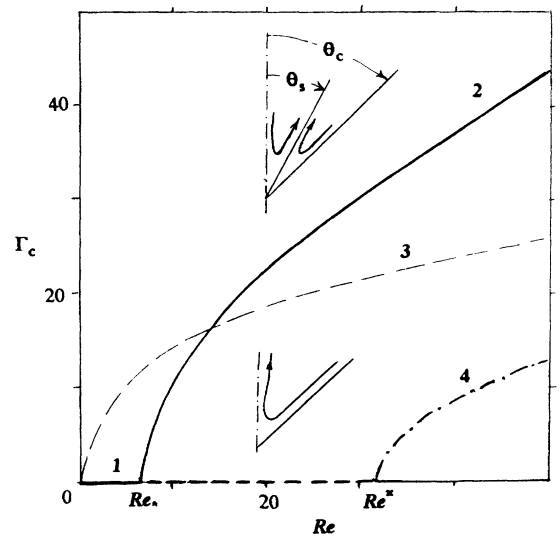

FIG. 4. Dependence of circulation Γ_c on the surface on the Reynolds number for the primary (1) and secondary (2) solutions. Curve 3 separates one- and two-cell regimes (see inserted sketches) and curve 4 is the collapse boundary. $\theta_c = 45°$.

recirculation zone appears leading to a two-cell regime.

This separation means that the axial velocity v_{ra} becomes negative. This is shown in Fig. 5 where $\mathrm{Re}_a = r v_{ra}/\nu$ is plotted as a function of Re for the primary (curve 1) and the self-rotation (curve 2) regimes. For the primary region, Re_a grows monotonically as Re increases and becomes infinite as $\mathrm{Re} \to \mathrm{Re}^*$ (the asymptote $\mathrm{Re} = \mathrm{Re}^*$ is shown). However, for the self-rotation regime, Re_a starts decreasing just after the bifurcation and changes its sign at $\mathrm{Re} = 13$. The dependence of θ_s, the angle of the conical surface separating the recirculation cells (see the upper sketch in Fig. 4), on Re is shown by curve 2′ in Fig. 5 for $\mathrm{Re} > 13$.

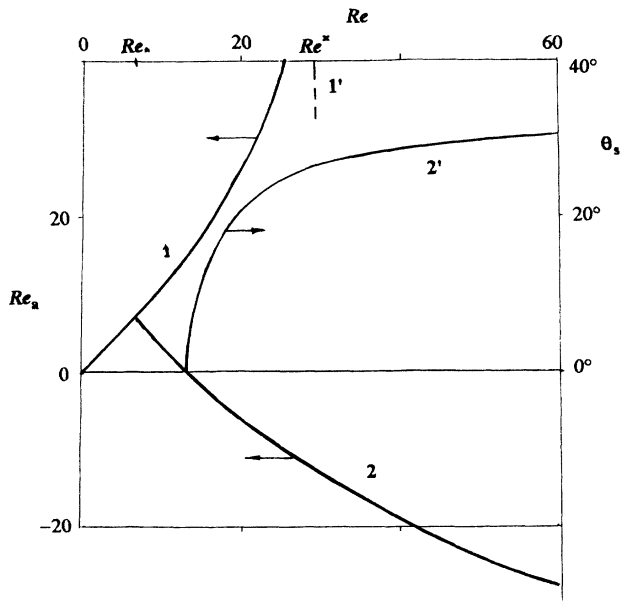

FIG. 5. Dependence of the radial velocity at the axis (Re_a) and separation angle θ_s (see Fig. 4) on Re for the primary (1) and the secondary (2,2′) solutions. $\theta_c = 45°$. 1′ corresponds to the collapse value $\mathrm{Re} = \mathrm{Re}^*$.

Unlike the primary solution, the swirling regime can be extended to arbitrarily large Re. We have made the calculations up to $\mathrm{Re} = 400$, the results for which are shown in Fig. 6. We choose this value because it corresponds to the experimentally recorded Re for swirling motion [4]. The observed angular velocity is near 100 Hz, and taking into account that the capillary diameter is 1 mm and $\nu = 10^{-6}$ m^2/sec (water), one obtains $\Gamma_c = 314$. Our calculations at $\mathrm{Re} = 400$ yield $\Gamma_c = 213$, which agrees well with experiments within an order of magnitude. As the experimental results are only estimates and not measured values, the agreement may be judged as good.

The value $\mathrm{Re} = 400$ is large enough for the formation of an inviscid core near the axis and a boundary layer near the cone surface; these are evident in Fig. 6. This figure shows that the core occupies approximately half of the angle interval considered and corresponds to a potential nonswirling inflow with a nearly uniform distribution of the radial velocity. This potential solution

$$\psi_p = -[-F''(1)]^{1/2}(1-x)$$

follows from (3), (6), and (7) after substituting $\Gamma \equiv 0$ and neglecting the linear terms in the left-hand side of (7). The near-surface boundary layer consists of an outward flow (fan jet) from the cone apex centered near $\theta = \theta_s = 36.5°$ and inflows on both sides of the jet. Thus, for large Re, the rotation and the outflow are localized in a near-surface boundary layer.

Although the experiment definitely shows rotational motion, there is no experimental evidence of the near-axis separation and inflow predicted by our theory. Possibly, the inflow does occur but cannot be observed by the visualization technique used in the experimental study. We feel that additional experiments involving velocity measurements are necessary for obtaining an experimental evidence of this separation.

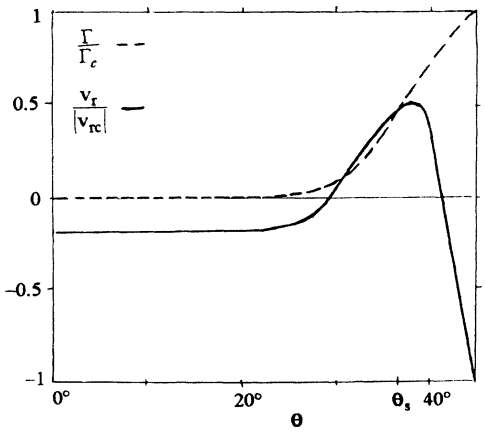

FIG. 6. Angular distribution of the normalized radial velocity ($v_r/|v_{rc}|$, solid curve) and circulation (Γ/Γ_c, broken curve) at $\mathrm{Re} = 400$. $\theta_s = 36.5°$ is the boundary between the recirculation cells. $\theta_c = 45°$.

V. DISCUSSION

Thus, we have found that the "trivial" solution corresponding to nonswirling steady axisymmetric laminar flow can undergo bifurcation into a swirling flow without the influence of any external body or surface sources of swirl. This result needs to be discussed in a more general context—the so-called problem of vortex dynamo, i.e., swirl generation, in nature and technology. The question arises: Is the rotation merely a consequence of initial conditions or is there some mechanism which generates rotation (dynamo)?

Rotation, as a consequence of initial conditions, can occur in the flow considered here if there is a weak rotation at the boundaries. In such a situation, the converging motion of the fluid will accentuate the weak rotation without any contribution from instabilities. However, under certain favorable conditions, instabilities cause symmetry breaking in the form of a dynamo. This possibility of the establishment of a laminar axisymmetric hydromagnetic dynamo was shown in [12] and, for turbulent flows, a vortex axisymmetric dynamo was reported in [9,10]. In the present study, a laminar vortex dynamo is obtained; however, this needs interpretation.

At first sign, this vortex dynamo seems to contradict the maximum principle for circulation in an axisymmetric flow with a given meridional velocity field. The principle requires the circulation to be the maximum at the boundary, and if $\Gamma=0$ at the boundary, then self-rotation is impossible. However, in the problem analyzed above, a different condition—zero azimuthal shear stress, $\tau_{\theta\phi}=0$—is applied at the surface. While this condition admits the trivial solution $\Gamma\equiv 0$, it also admits a nontrivial solution. In this solution, Γ is maximum at the cone boundary in accordance with the maximum principle. However, the boundary does not serve as a source of swirl here. Note that the important limitation is that the self-rotation can occur only for cones with angle $\theta_c<90°$ which corresponds to a convex liquid surface.

Additionally, it might appear that the laminar vortex dynamo contradicts the Cowling "antidynamo" theorem [13]. However, it should be noted that Cowling's theorem, which claims the impossibility of axisymmetric self-generation of magnetic field (analogous to the generation of swirl here), includes the condition that the magnetic field decays as r^{-3}. For the conical similarity class considered here, this condition is not satisfied since the velocity decays $\sim 1/r$ and there is a nonzero circulation as $r\to\infty$. Thus, a vortex dynamo is feasible.

This observed bifurcation of the self-similar swirling regime can be interpreted as a result of either a spatial or a temporal instability. We can expect that for small Reynolds numbers the regime without swirl is stable. According to the general theory of bifurcations [14], after a supercritical pitchfork bifurcation, the primary regime loses stability and the secondary regime is stable. Note that a detailed analysis of stability problems requires finding the solution of non-self-similar, (at least) two-dimensional problems; this is difficult even for the linear case. In the case of spatial instability, one can consider the transport of an outer rotation to the inner region of self-similarity. If the circulation Γ_0 is given at $r=r_0$ and a similarity region (SR) exists for $r_i<r<r_0$, it is expected that at $\mathrm{Re}<\mathrm{Re}_*$, the circulation will decay to zero in some neighborhood of $r=r_0$ and will be absent in the SR. However, for $\mathrm{Re}>\mathrm{Re}_*$, circulation is transported inside the SR and reaches a value Γ_c corresponding to the self-similar solution. It is important to note that Γ_c depends on Re but not on Γ_0. In such an interpretation, the bifurcation found implies a strong concentration of angular momentum in a small region of physical space; this may be important for technical applications and predictions of natural phenomena.

In the temporal case, as mentioned in the Introduction, establishment of swirling secondary regimes can be related to nonsimilar unsteady disturbances with regions having different signs of circulation. If the "negative" region is positioned near the outer boundary (say, the rim of the capillary tube), then the boundary absorbs a negative angular momentum, and the positive circulation becomes dominant in the flow. We consider this to be more appropriate for rotation in the Zeleny-Taylor cones.

Possible applications of the self-rotation phenomenon include electrosprays which are used in a variety of rapidly growing industries—from paint spraying and jet printing to fuel atomization and biotechnology. Here we would like to speculate on possible meteorological applications. Clouds have been known to have conical forms just before generation of tornadoes. A draft of cold air can induce a convergent motion near the cloud surface and create conditions favorable to self-rotation. Similar conditions leading to the development of whirlpools can occur in low pressure regions of oceans (causing a convex ocean surface) with thermoconvection instability (providing an ascending air flow) which induces radial converging winds that, in turn, drive a converging motion of water near the ocean surface.

ACKNOWLEDGMENTS

We are grateful to Shashi Menon for help in the preparation of this manuscript and to the Air Force Office of Scientific Research for support through Grant No. F49620-92-J-0200.

[1] K. E. Torrance, J. Fluid Mech. **95**, 477 (1979).
[2] M. Kawakubo, Y. Tsuchia, M. Sugaya, and K. Matsumura, Phys. Lett. A **68**, 65 (1978).
[3] M. Funakoshi and S. Inoue, J. Fluid Mech. **192**, 219 (1988).
[4] J. Fernandez de la Mora, J. Fernandez Feria, and A. Barrero, Bull. Am. Phys. Soc. **36**, 2619 (1991); and (unpublished).
[5] J. Zeleny, Phys. Rev. **10**, 1 (1917).
[6] G. I. Taylor, Proc. R. Soc. London Ser. A **280**, 383 (1964).

[7] I. Hayati, A. I. Bailey, and Th. F. Tadros, Nature **319**, 41 (1986).
[8] M. A. Goldshtik, V. N. Shtern, and E. M. Zhdanova, Dokl. Adad. Nauk SSSR **277**, 615 (1984) [Sov. Phys.—Dokl. **277**, 815 (1984)].
[9] M. A. Goldshtik and V. N. Shtern, Proc. R. Soc. London Ser. A **419**, 91 (1988).
[10] M. A. Goldshtik and V. N. Shtern, J. Fluid Mech. **218**, 483 (1990).
[11] J. Fernandez de la Mora, J. Fluid Mech. **243**, 561 (1992).
[12] M. A. Goldshtik and V. N. Shtern, Zh. Eksp. Teor. Fiz. **49**, 266 (1989) [Sov. Phys. JETP **96**, 1728 (1989)].
[13] H. K. Moffatt, *Magnetic Field Generation in Electrically Conducting Fluids* (Cambridge University, Cambridge, England, 1978).
[14] M. Golubitsky and D. G. Schaeffer, *Singularities and Groups in Bifurcation Theory* (Springer-Verlag, New York, 1985).